Wireless Pers Commun (2015) 84:2815–2833
DOI 10.1007/s11277-015-2768-5

Improvement in the Performance of WiMAX with Channel Equalizers and Space Time Block Coding Techniques Using Simulink

B. Siva Kumar Reddy[1] · **B. Lakshmi**[1]

Published online: 28 May 2015

Abstract WiMAX is a coming forth broadband wireless technology that considered as one of the most prominent solution to provide high speed data services. This paper addresses the design of WiMAX end to end physical layer (PHY) in Simulink with channel equalization and space time block coding techniques. The authors analyzed the performance of WiMAX PHY with decision feedback equalizers (DFE), linear equalizers and blind equalizers over AWGN and multipath faded channels. Results include MISO channel power spectral density (PSD), antenna amplitude/PSD/phase difference, multipath faded and AWGN channel's effect on the transmitted signal and the performance of proposed equalizers on the received signals. This paper concluded that the linear equalizers have higher frame error rates (FER) than DFE. However, blind equalizers have higher FERs compared to conventional equalizers with better spectral efficiency as they need no training sequence.

Keywords BER · Channel equalizers · FER · OFDM · Simulink · STBC · WiMAX

1 Introduction

The The experienced growth in the use of digital networks has led to the need for the design of new communication networks with higher capacity. Wireless digital communications are an emerging field that has experienced an spectacular expansion during the last several years. Moreover, the huge uptake rate of mobile phone technology, Wireless Local

✉ B. Siva Kumar Reddy
bsivakumar100@gmail.com

[1] Department of Electronics and Communication Engineering, National Institute of Technology Warangal, Warangal 506004, Andhra Pradesh, India

Area Network (WLAN) and the exponential growth of Internet have resulted in an increased demand for new methods of obtaining high capacity wireless networks [1].

Worldwide interoperability for microwave access (WiMAX) [2] was designed to offer broadband wireless access (BWA) services [3] to metropolitan areas providing users with larger coverage ranges and higher data rates. WiMAX applied orthogonal frequency division multiplexing (OFDM) [4] to provide high data rates with better spectral efficiency. The purpose of choosing OFDM (multicarrier system) over a single carrier systems is its capability to preserve the adverse and harsh channel conditions. OFDM additionally improves the data rate and reduces the fading effect of channel. Orthogonal frequency division multiple access (OFDMA) [4] is involved in BWA services due to its capability to persist multipath interference. In the BWA services, signals have to be transmitted through time dispersive channels [5] for communication.

Time dispersive channels may result an inter symbol interference (ISI) [6], a type of distortion that induces symbols to overlap and get to be indistinguishable by the receiver. For instance, the receiver encounters postponed adaptations of a symbol transmission which can interfere with other symbol transmissions in a multipath faded environment. An equalizer [7] is attempted at the receiver end to mitigate ISI with improved receiver performance. The equalizers have been classified into two types in terms of their usage and execution such as linear and non-linear [8]. Linear equalizers are further classified into two types such as symbol-spaced equalizers and fractionally spaced equalizers (FSEs). Linear equalizers are reasonably and computationally simple, while non-linear equalizers are unpredictable and computationally tough. The simplicity of linear equalizers takes on at a cost of execution. Then again, non-linear equalizers have higher execution complexity, yet they offer prevalent execution. Decision feedback equalizer [8] gives a decent tradeoff in the middle of execution and complexity. Linear and decision-feedback equalizers called as adaptive equalizers [9] because of using an adaptive algorithm. Authors proposed various adaptive algorithms to implement WiMAX physical layer are Least Mean Square (LMS), Signed LMS, Normalized LMS, Variable step-size LMS, Recursive Least Squares (RLS) and Constant Modulus Algorithm (CMA) [10]. The selection procedure of an algorithm among these many algorithms is presented in Sect. 3.

Fading might be reduced by utilizing receiver and transmit diversity [11], there by enhancing the reliability of the transmission link. In diversity techniques [12], same data is transmitted across independent fading channels to avoid fading and co-channel interference [13] essentially.

2 Channel Equalization

Equalization is the process of recovering the data sequence from the undetermined channel samples. Here will be a few generalizations that may impact the determination of particular adaptive algorithm such as LMS algorithm [14] rapidly however converges slowly, and its complexity increases linearly with the number of weights. To simplify hardware implementation, the various types of signed LMS algorithms are proposed. The Normalized LMS and variable-step-size LMS algorithms are more robust to variability of the input signal's statistics (such as power). The RLS algorithm [15] converges quickly, but its complexity increases with the square of the number of weights. This algorithm can also be unstable when the number of weights are more. The constant modulus algorithm (CMA) is

useful for constant modulus modulations such as PSK and it needs no training sequence. However, if CMA has no extra side data, it may introduce phase ambiguity. For instance, CMA might find weights that generate a perfect QPSK constellation but may result a phase rotation of 90, 180, or 270 degrees. On the other hand, differential modulation might be utilized to avoid phase ambiguity.

All the proposed equalizers implement a symbol-spaced (i.e. T-spaced) equalizer when the user sets the 'Number of samples per symbol' parameter to 1 and otherwise, the block implements a fractionally spaced equalizer.

2.1 Decision Feedback Equalizer

A fundamental structure of the decision feedback equalizer (DFE) [8] is presented in Fig. 1. The DFE comprises of a transversal feed forward and feedback filter. The DFE utilizes past corrected samples, w(n), from a decision device to the feedback filter and consolidates with the feed forward filter. Basically, the role of feedback filter is to mitigate the ISI raised by formerly detected symbols from the estimates of future samples. Assume that the DFE is updated with a recursive algorithm; the feed forward filter weights and feedback filter weights might be together adjusted by the LMS algorithm on a common error signal $\hat{e}(n)$ as appeared

$$W(n+1) = W(n) + \mu\hat{e}(n).V(n), \tag{1}$$

where $\hat{e}(n) = y(n) - z(n)$, $V(n) = [x(n), x(n-1), \ldots x(n-k1-1), y(n-k2-l)]^T$. The feed forward and feedback filter weight vectors are indicated in a joint vector as $W(n) = \left[w_0(n), w_1(n), \ldots, w^n_{k1+k2-1}\right]^T$. $k1$ and $k2$ indicate the feed forward and feedback filter tap lengths separately. Generally, the DFE is called as a non-linear equalizer due to non linear behaviour of the decision device. Be that as it may, the DFE structure is still a linear combiner and the adaptation loop is also linear. In this way, it has been presented as a linear equalizer structure.

2.2 Symbol-Spaced Equalizers

A symbol-spaced linear equalizer [8] comprises of a tapped delay line that stores samples from the input signal. When for every symbol period, the equalizer yields a weighted sum of the values in the delay line and adjusts the weights to get ready for the next symbol period. As the sample rates of the input and output are equal, this kind of equalizer is called symbol-spaced equalizer.

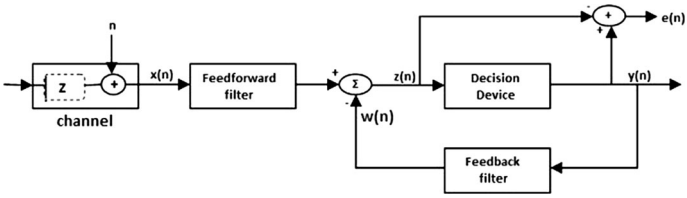

Fig. 1 Decision feedback equalizer (DFE)

3 Adaptive Fir Algorithms

As demonstrated in Fig. 2, a sample from a digital input signal x(n) is fed into a device, called an adaptive filter [16], that processes a respective output signal sample $y(n)$ at time n.

In general, an adaptive FIR filtering algorithm is expressed as

$$W(n+1) = W(n) + \mu(n)G(e(n), X(n), \phi(n)), \tag{2}$$

where $\mu(n)$ is a step size parameter, $G(-)$ is a specific vector-esteemed nonlinear function, $X(n)$ and $e(n)$ are the input signal vector and error signal, respectively, and $\Phi(n)$ is a vector of states that stores a pertinent data about the characteristics of the input and error signals and/or the coefficients at previous time instants. In the simplest algorithms, $\Phi(n)$ is not utilized, and the main data required to change the coefficients at time n are the error signal, input signal vector, and step size.

The mean-squared error (MSE) cost function as

$$J_{MSE}(n) = \frac{1}{2}\sum_{-\infty}^{\infty} e^2(n).P_n(e(n))de(n) \tag{3}$$

$$= \frac{1}{2}Ee^2(n), \tag{4}$$

where $P_n(e)$ indicates the probability density function of the error at time n and $E-$ is shorthand for the *expectation integral* on the right-hand side of Eq. (3). It empowers us to focus both the optimum coefficient values given knowledge of the statistics of d(n) and x(w) a basic iterative technique for adjusting the parameters of a FIR filter.

3.1 LMS Algorithm

The cost function $J(n)$ picked for the steepest descent algorithm decides the coefficient result got by the adaptive filter. One such cost function is the minimum-squares cost function given by

$$J_{LS}(n) = \sum_{k=0}^{n} \alpha(k)\big(d(k) - W^T(nX(k))\big)^2, \tag{5}$$

where $a(n)$ is a suitable weighting succession for the terms inside the summation.

On the other hand, we can propose the simplified cost function $J_{LMS}(n)$ given by

$$J_{LMS}(n) = \frac{1}{2}e^2(n). \tag{6}$$

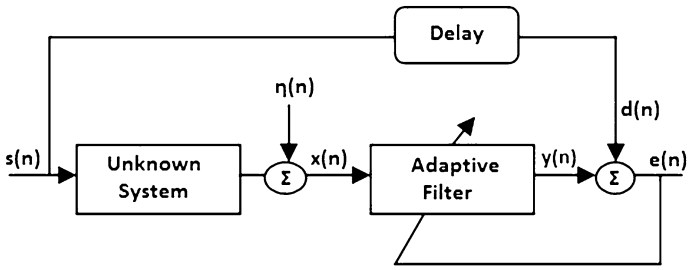

Fig. 2 Adaptive system identification

This cost function might be considered as an instantaneous estimate of the MSE cost function, as $J_{MSE}(n) = E_{JLMS}(\mathrm{n})$. Bringing derivatives of $J_{LMS}(n)$ as for the elements of $W(n)$ from ref [9], we acquire the LMS adaptive algorithm as

$$W(n+1) = W(n) + \mu(n)e(n)X(n). \tag{7}$$

Note that this algorithm is the general form of Eq. (2). It additionally requires just augmentations and increases to execute. Indeed, the number of operations required for the LMS algorithm is about the same as the FIR filter structure with fixed coefficient values, which is one of the reasons for the algorithm's popularity.

3.2 RLS Algorithm

Rather than the LMS algorithm, the RLS algorithm utilizes data from all past input samples (and not just from the current tap-input samples) to estimate the (inverse of the) auto-correlation matrix of the data vector. To decline the impact of input samples from the far past, a weighting factor for the impact of each sample is utilized. This weighting factor is presented in the cost function

$$J[n] = \sum_{i=1}^{n} \rho^{n-i} |e[i,n]|^2, \tag{8}$$

where the error signal $e_i[i,n]$ is figured for all times $1 \le i \le n$ utilizing the current filter coefficients $c[n] : e[i,n] = d[i] - c^T[n]x[i]$, where $x[i]$ and c^T denotes input signal and transpose of the channel coefficient vector respectively. At the point when $\rho = 1$, the squared error for all sample times i up to current time n is considered in the cost function J equally. In the event that $0 < \rho < 1$ the impact of past error values decays exponentially: method of *exponentially weighted least squares* is called the *forgetting factor*. Analogous to the determination of the LMS algorithm we find the gradient of the cost function with respect to the current weights

$$J[n] = \sum_{i=1}^{n} \rho^{n-i}\big(-2E(d[i]x[i]) + 2E(x[i]x^T[i])c[n]\big). \tag{9}$$

The resulting equation for the optimum filter coefficients at time n is

$$\phi[n].c[n] = z[n] \tag{10}$$

$$c[n] = \phi^{-1}[n].z[n], \tag{11}$$

with $\phi[n] = \sum_{i=1}^{n-i} x[i].x^T[i]$, $z[n] = \sum_{i=1}^{n} \rho^{n-i} d^* x^T[i]$ Both $\phi[n]$ and $z[n]$ can be computed recursively:

$$\phi[n] = \rho\phi[n-1] + x[n]x^T[n], \tag{12}$$

and

$$z[n] = \rho z[n-1] + d^T[n]x[n]. \tag{13}$$

To find $c[n]$ the coefficient vector we, however, need the inverse matrix $\phi^{-1}[n]$. Using a matrix inversion lemma [19] a recursive update equation for $P[n] = \phi^{-1}[n]$ is found as:

$$P[n] = \rho^{-1}P[n-1] + \rho^{-1}k[n]x[n], \tag{14}$$

with

$$k[n] = \frac{\rho^{-1}P[n-1]x[n]}{1 + \rho^{-1}x^T[n]P[n-1]x[n]}. \tag{15}$$

Finally, the weights update equation is

$$c[n] = c[n-1] + k[n]\big(d^T[n] - x^T[n]c[n-1]\big). \tag{16}$$

The mathematical statements to solve in the RLS algorithm at each time step are (15) and (16). The RLS algorithm is computationally more complex than the LMS algorithm. The RLS algorithm regularly demonstrates a faster convergence compared to the LMS algorithm.

3.3 Blind Equalizer

The block diagram of blind equalization system model is depicted in Fig. 3. Let's assume that the transmitted sequence $a(k)$ is the symbol sequence of independent identical distribution(i.i.d), and $a(k) \in A$. Where A is the windows character set. The sampled input to the equalizer can be defined as $x(k) = [a(k) * h(k)] + n(k)$, where $a(k) = a_R(k) + ja_I(k)$ is the data symbol that was sent, $h(i)$ is the baseband equivalent channel impulse response, $'*'$ indicates discrete convolution, $n(k)$ is complex Gaussian noise. Where $f(k)$ and $X(k)$ are the tap weight vector and the input data vector of the equalizer at k^{th} instant sampling time respectively.

The baseband channel is a column vector of size $N_c \times 1$ and can be written as

$$C(k) = [c(k) + c(k+1), \ldots, c(K + N_c - 1)]^T. \tag{17}$$

The equalizer is a column vector of size $N_f \times 1$ and can be written as

$$f(k) = [f(k) + f(k+1), \ldots, f(K + N_f - 1)]^T. \tag{18}$$

Z(k) is a column vector of size $N_s \times 1$ of the input data sequence at time instant k , i.e.

$$Z(k) = [z(k) + z(k+1), \ldots, z(K + N_c - 1)]^T. \tag{19}$$

At time instant k, the received data sequence of equalizer is given by

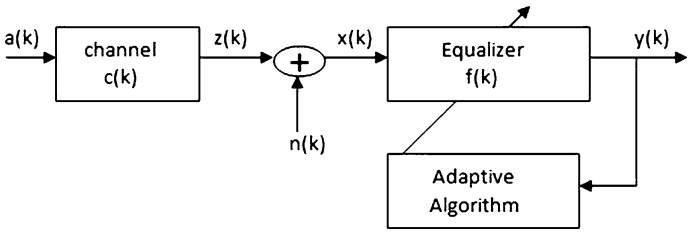

Fig. 3 Blind equalization model

$$x(k) = C^T(k) \cdot a(k) + n(k) \tag{20}$$

$$= \sum_{i=0}^{N_c} C(i)a(k-i) + n(k). \tag{21}$$

The output of the equalizer at sample k is expressed as

$$y(k) = f^T(k)X(k) \tag{22}$$

$$= \sum_{j=0}^{N_f} f(j)y(k-j). \tag{23}$$

3.3.1 CMA Equalizer

The constant modulus algorithm (CMA) is a blind equalizer, but it only works on signals that have a constant amplitude, or modulus. The CMA algorithm accepts the number of taps to use in the equalizer, which will be based on some combination of known best practices, and some actual knowledge of the channel itself. We need to keep this number as small as possible to reduce the overhead of the algorithm after verifying that there is sufficient degree of opportunity to correct channel. In the case of blind equalization, the specified data symbol isn't available. For this case, equalizer taps are restored utilizing an algorithm that minimizes a particular error function. The error function will be made by observing the equalizer output and utilizing some priori details about sent data constellation statistics. The error function that is reduced in this instance of the Godard algorithm and that is a special case of Bussgang class cost function is [20]

$$J(k) = \frac{1}{4}(|y(k)|^2 - R)^2, \tag{24}$$

where $R = E\{|a(k)|^4\}/E\{|a(k)|^2\}$ is an appropriately selected constant that based on the transmitted information statistics. To minimize an error function, blind equalization algorithms can be expressed as below.

$$\begin{aligned} f(k+1) &= f(k) + \mu y(k)(|y(k)|^2 - R)X^*(k) \\ &= f(k) + \mu y(k)e(k)X^*(k), \end{aligned} \tag{25}$$

where μ is a step-size, and $0 < \mu \leq 1$. The step size (μ) may be calculated by rule of thumb as given by

$$\mu = \frac{1}{5(2N+1)P_R} \tag{26}$$

where, N is the equalizer length, P_R is the received power that can be estimated in the receiver.

The error signal $e(k)$ is given by

$$e(k) = |y(k)|^2 - R. \tag{27}$$

Equation (25) is viewed as CMA (constant modulus algorithm).

4 Space Time Block Code (STBC)

STBC [17] can accomplish full transmit diversity providing maximum likelihood decoding algorithm built just with respect to linear processing at the receiver. The new transmit diversity scheme was presented by Alamouti known as Alamouti scheme [18]. This scheme utilizes two transmit antenna (N_t) and one receive antenna(N_r) and can have a maximum diversity order of $2N_r$. Alamouti scheme has the rate of unity i.e. full rate since it transmits two symbols after every two time periods. This scheme is effective in all the applications where system capacity is limited by multipath fading.

Let us assume a signal x_1 and x_2 are transmitted by antenna 1 and antenna 2 respectively at time t. At next time $t + T$, signal $-x_2^*$ is transmitted from antenna 1 and signal x_1^* is transmitted from antenna 2 where (*) is the complex conjugate operation. Let h_1 and h_2 be the channel response for antenna 1 and antenna 2. Assume α_1 and α_2 be the individual path gains from transmit antenna 1 and 2 to the receive antenna as given by expression

$$h_1 = \alpha_1 e^{j\theta_1} \tag{28}$$

$$h_2 = \alpha_2 e^{j\theta_2}, \tag{29}$$

Let y_1 and y_2 be receiving signal at a receiver in time t and t + T respectively.

$$y_1 = y(t) = h_1 x_1 + h_2 x_2 + n_1 \tag{30}$$

$$y_2 = y(t+T) = -h_1 x_2^* + h_2 x_1^* + n_2, \tag{31}$$

where n_1 and n_2 are variable representing noise (AWGN, fast fading).

The combiner combines the two signals as,

$$\hat{x}_1 = h_1^* y_1 + h_2 y_2^* \tag{32}$$

$$\hat{x}_2 = h_2^* y_1 - h_1 y_2^*. \tag{33}$$

Now by substituting above two equations in combiner equation, the result is

$$\hat{x}_1 = (\alpha_1^2 + \alpha_2^2) x_1 + h_1^* n_1 + h_2 n_2^* \tag{34}$$

$$\hat{x}_2 = (\alpha_1^2 + \alpha_2^2) x_2 + h_2^* n_1 - h_1 n_2^*, \tag{35}$$

These combined signals are then send to the maximum likelihood detector which makes a decision for each of the signals x_1 and x_2 to select.

5 System Model

Simulink gives an effective augmentation to Matlab for modeling and simulating many types of systems particularly communication systems. Matlab and Simulink are utilized for demonstrating WiMAX OFDM transmitter as presented in [21].

The WiMAX standard gives particular instantiations of the physical layer data vectors (*Input_data*, *randomized_data*, *ReedSolomoncoding_data*, and *Interleaved_data*) for distinctive code rates (concatenated Reed Solomon and Convolutional Coding) and modulation schemes (M-QAM, QPSK) are distributed as case studies [21]. To ensure

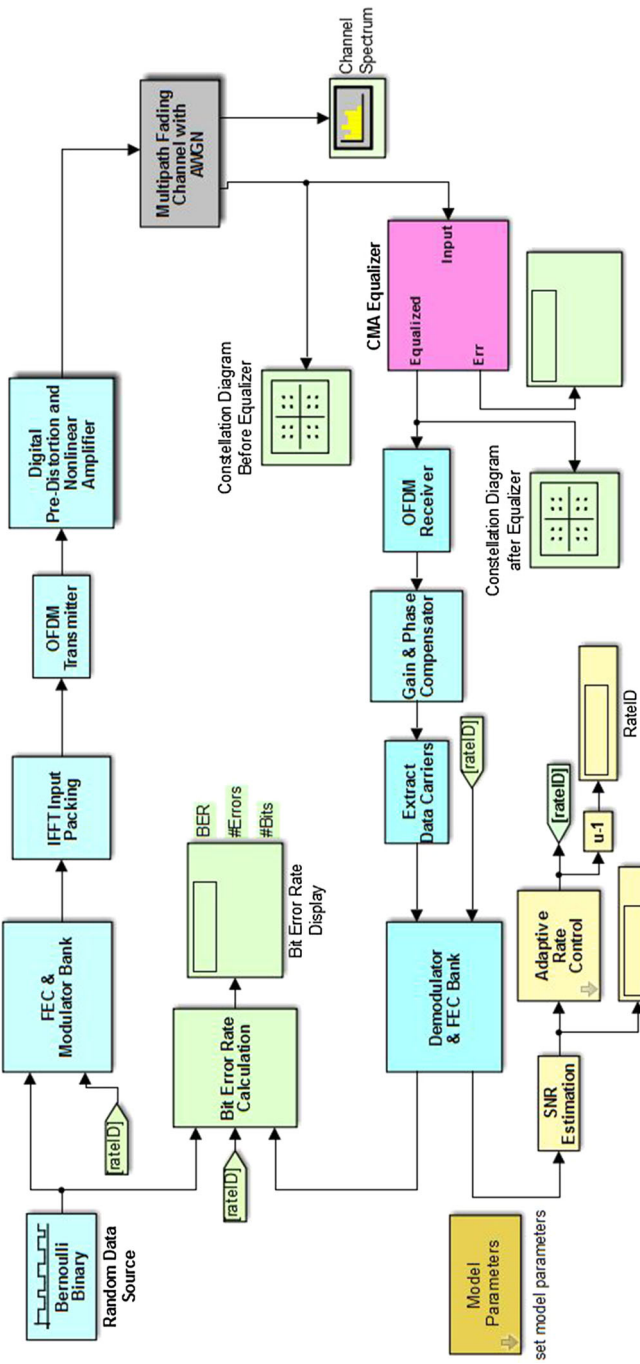

Fig. 4 WiMAX PHY layer With CMA equalizer for SISO model

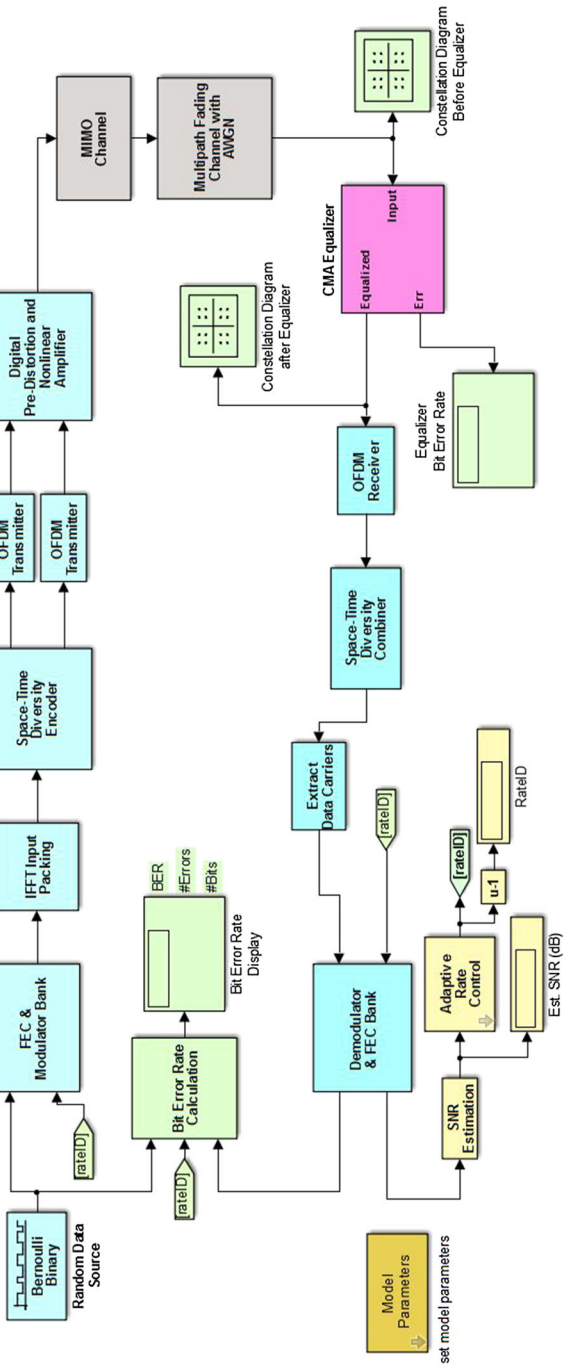

Fig. 5 WiMAX PHY layer including STBC and With CMA equalizer

proper implementation, the end-to-end system was modeled as per the standard [22] for this particular configuration.

In this paper, authors presented the main components of the WMAN 802.16-2004 OFDM physical layer utilizing two models: one without STBC for SISO and two with STBC for MISO (shown in Figs. 4, 5 respectively). Both models included all the mandatory coding and modulation options. The tasks performed in the system models are: Random bit data Generation that makes a downlink burst comprises of a number of OFDM symbols; Forward Error Correction (FEC), comprising of a Reed-Solomon (RS) outer code concatenated with a rate-compatible inner convolutional code (CC); Data interleaving; Modulation, utilizing one of the BPSK, QPSK, 16-QAM or 64-QAM constellations specified (in this paper, 16QAM is used); OFDM transmission utilizing 192 sub-carriers, 8 pilots, 256-point FFTs, and a variable cyclic prefix length; STBC utilizing an Alamouti code; A single OFDM symbol length preamble that is utilized as the burst preamble. For the optional STBC model, both antennas transmit the single symbol preamble; An optional memoryless nonlinearity that might be determined at several backoff levels. An optional digital pre-distortion capability that corrects for the nonlinearity; A Multiple-Input-Single-Output (MISO) fading channel with AWGN for the STBC model; OFDM receiver that incorporates channel estimation utilizing the inserted preambles. For the STBC model, this implies diversity Both models also used an adaptive-rate control scheme based on SNR estimates at the receiver to vary the data rate dynamically based on the channel conditions. The models used the standard-specified set of seven rates for OFDM-PHY, each corresponding to a specific modulation and RS-CC code rate as denoted by Rate_ID (see the Table 1).

Besides, both models incorporate blocks for measuring and showing the bit error rate after FEC, the channel SNR and the *Rate_ID*. Spectrum Analyzer blocks display the spectra of both the OFDM transmitter output and the faded AWGN channel output. Additionally, a Scatter Plot scope shows the AM/AM and AM/PM characteristics of the signal at the output of the memoryless nonlinearity. At last, a Scatter Plot scope shows the received signal, helping us to illustrate channel impairments and modulation adaptation as the simulation runs.

The Model Parameters setup block (shown in Figs. 4, 5) permits us to select and determine system parameters, such as number of OFDM symbols per burst, channel bandwidth and the cyclic prefix factor. Differing these parameter values provides us to experiment with the different WiMAX profiles as defined by the WiMAX Forum [22], and gauge the system performance for each.

Table 1 Modulation scheme selection basis on Rate_ID value

Rate ID	Modulation RS-CC rate
0	BPSK 1/2
1	QPSK 1/2
2	QPSK 3/4
3	16QAM 1/2
4	16QAM 3/4
5	64QAM 1/2
6	64QAM 3/4

6 Simulation Results

The WiMAX physical layer is designed in Simulink to plot MISO channel PSD, Antenna amplitude, Antenna PSD, Antenna phase difference, multipath faded and AWGN channel's effect on the transmitted signal and proposed equalizers performance on the received signals. The frame error rate (FER) values of proposed equalizers such as LMS Linear equalizer, NLMS Linear, RLS Linear, Sign LMS Linear, Variable Step LMS Linear, Variable Step LMS DFE, RLS DFE, Sign LMS DFE, LMS DFE, NLMS DFE, CMA and MSLE equalizers are noted in Tables 2 and 3. The Simulink model which is used to get equalizer performance in terms of FER on 16QAM signal is shown in Fig. 6. Results are observed by changing channel as multipath fading and AWGN are noted in Tables 2 and 3 respectively. It can be concluded from the Tables 2 and 3 that linear equalizers have higher FER values compared DFE equalizers. The CMA and MLSE equalizers (blind equalizers) showed higher FER values compared to remaining all considered equalizers as they did not use any training sequence. Blind equalizers (CMA and MLSE) have higher FER values at low SNRs and low FERs at high SNRs. Hence, Blind equalizers are useful at high SNRs. The Fig. 7 presents the scatter plots for Variable Step LMS, RLS DFE, MLSE equalizers at 20 and 50 dB SNRs. The Fig. 7a shows the signal transmitted over multipath faded channel. The received faded signal is passed through Variable Step LMS DFE, RLS DFE and MLSE equalizers at 20 dB SNR and presented in Fig. 7b, c and d separately. The scatter plot pointed at Fig. 7e is captured at 50 dB SNR for Variable LMS DFE equalizer. It can be concluded from the Fig. 7 that the signal constellation is improved as SNR increases and the MLSE equalizer provided the best constellation compared to remaining cases and also Variable LMS Linear equalizer expressed better constellation than RLS DFE.

The channel output spectrum captured for without STBC and with STBC models are presented in Fig. 8a, b respectively. Due to two transmitted signals in STBC case, the channel output plot has two spectra. Coming to the model that shown in Fig. 4, the channel

Table 2 FER values noted for 16QAM signal transmitted over multipath faded channel

Equalizer	SNR = 5 dB	10 dB	20 dB	30 dB	40 dB	50 dB
LMS linear	23.148	23.9233	22.2223	21.9777	23.2563	21.7865
NLMS linear	19.3798	21.6452	21.9297	21.3674	21.7865	21.053
RLS linear	17.3389	18.5531	18.3823	17.8891	18.2825	17.9856
Sign LMS linear	20.0010	20.04	20.9205	20.0001	20.4082	20.9205
Variable step LMS linear	15.3375	17.8253	17.3745	17.1527	18.6659	18.7969
Variable step LMS DFE	17.6016	19.0123	17.065	20.0404	19.3421	19.4553
RLS DFE	18.9756	19.8805	20.2837	19.7628	20.6185	20.4497
Sign LMS DFE	21.9777	20.3664	19.2679	22.0264	20.5759	20.2021
LMS DFE	19.0841	23.6406	18.4505	23.3102	19.0841	20.4497
NLMS DFE	19.92	21.3216	21.786	20.8333	20.4497	19.6424
CMA	54.0535	33.5574	45.6623	44.6413	44.6099	39.062
MLSE	40.729	57.8026	52.3569	44.8426	57.4718	57.8026

Table 3 FER values noted for 16QAM signal transmitted over AWGN channel (no fading)

Equalizer	SNR = 5 dB	10 dB	20 dB	30 dB	40 dB	50 dB
LMS linear	20.6614	23.5213	22.0264	23.6942	24.8142	21.7865
NLMS linear	21.8819	21.8814	21.4592	19.1204	22.472	22.0748
RLS linear	18.3487	19.4177	17.2414	16.2867	18.5186	19.1939
Sign LMS linear	16.2338	20.3668	21.1867	20.2081	18.083	20.3252
Variable step LMS linear	18.1491	19.4177	17.4827	19.2679	18.1491	19.3748
Variable step LMS DFE	16.4745	17.3612	16.2378	16.3933	16.9781	16.4745
RLS DFE	18.5186	20.1207	17.2713	19.3798	18.0834	18.5539
Sign LMS DFE	15.9489	20.4497	22.3714	21.8347	22.1733	20.5314
LMS DFE	22.0264	22.7273	21.6447	20.4082	21.1867	21.0085
NLMS DFE	21.053	20.7897	20.661	21.2315	21.7865	20.768
CMA	42.5529	43.2903	42.017	47.0012	43.8394	38.9101
MLSE	51.8139	57.8026	52.9114	58.8352	58.8252	57.1441

output signal (captured at 20 dB SNR, shown in Fig. 9) is applied as input to a CMA equalizer and it can be concluded that due to fading influence on the signal, multipath faded channel depicted more erroneousness in the scatter plot than AWGN channel. The influence of CMA equalizer on the channel output scatter plots are shown in Fig. 10. CMA equalizer outputs are captured at 5, 20 and 50 dB SNR values respectively and the scatter plots are improved by increasing SNRs. The scatter plots shown in Fig. 10 have better performance than shown in Fig. 9. Hence, it can be concluded that performance was improved by using a CMA equalizer.

The presented model in Fig. 4 is modified by introducing STBC to provide MISO services and included a MIMO channel as shown in Fig. 5. The effect of CMA equalizer on a STBC transmitted signal over multipath faded channel and AWGN channel (at 20 dB SNR) are presented in Figs. 11 and 12 respectively. It can be concluded that the scatter plots in the Fig. 11 have good performance than in Fig. 12 because of AWGN channel in Fig. 11.

AM-to-PM conversion is usually defined as the change in output phase for a 1-dB increment in the power-sweep applied to the amplifier's input (i.e. at the 1 dB gain compression point). It is expressed in degrees-per-dB. An ideal amplifier would have no interaction between its phase response and the power level of the input signal. In this paper, the AM/AM and AM/PM plots are used to determine how well the digital pre-distortion function compensates for the degradation induced by the memoryless nonlinearity. Ideally, the AM/AM curve should be linear, and the AM/PM characteristic should be horizontal as shown in Fig. 13. Since the nonlinearity induces a gain compression on the input signal, the pre-distortion applies a "gain expansion" on the signal, such that the composite gain is linear. However, the pre-distortion is effective only over the input amplitude range up to the peak of the AM/AM nonlinearity. We should see that the pre-distortion is only marginally effective when the input signal amplitude drives the amplifier heavily into saturation.

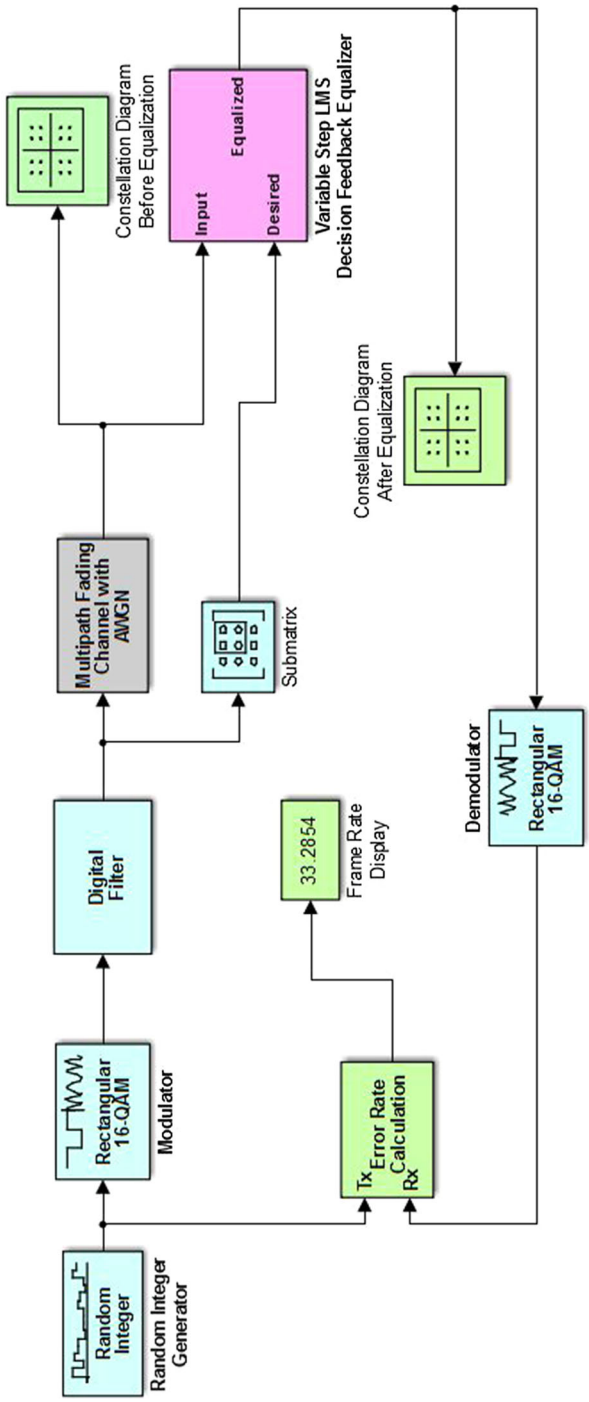

Fig. 6 Equalization block diagram

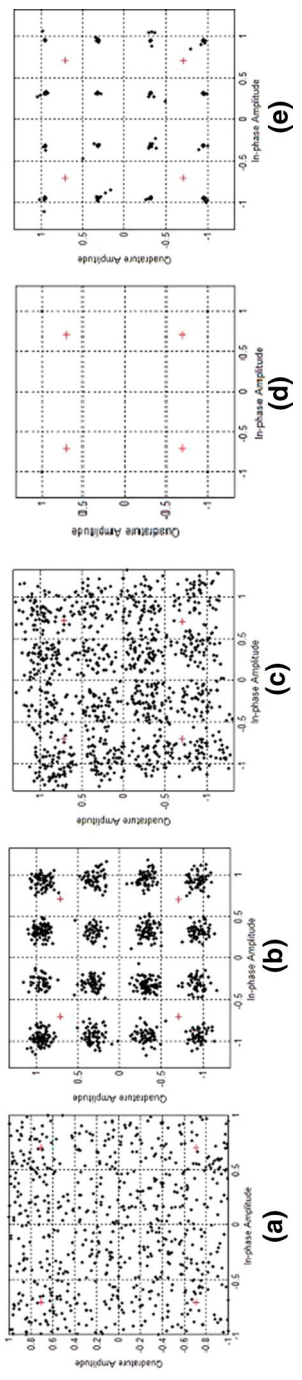

Fig. 7 Equalizer output scatter plots for **a** Multipath faded channel output, **b** variable step LMS DFE at 20 dB, **c** RLS DFE at 20 dB, **d** MLSE at 20 dB, **e** variable step LMS DFE at 50 dB

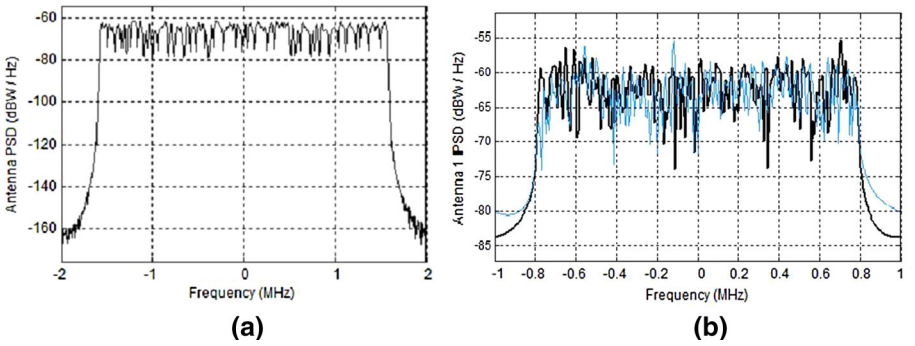

Fig. 8 Channel output spectrum **a** without STBC **b** with STBC

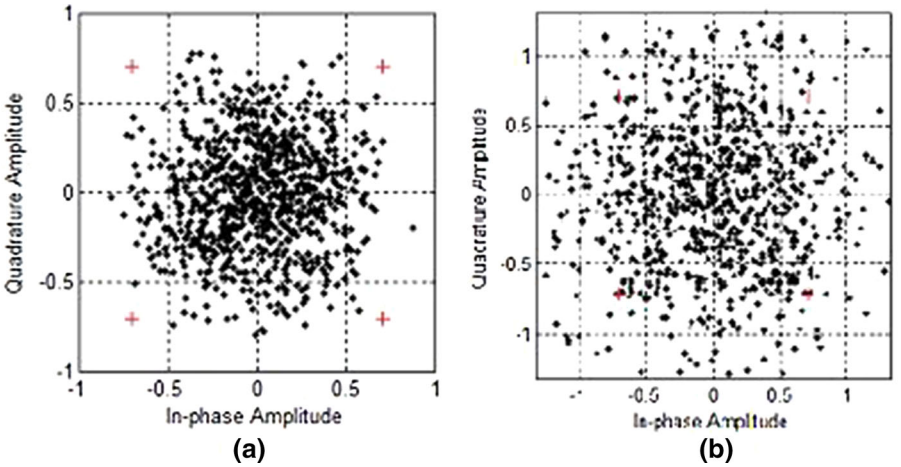

Fig. 9 Channel output scatter plots at 20 dB SNR **a** AWGN, **b** multipath faded channel

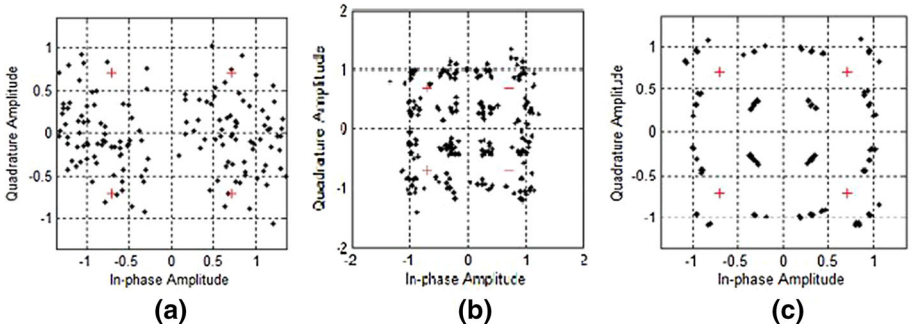

Fig. 10 CMA Equalizer output scatter plots (without STBC) at different SNRs **a** 5 dB, **b** 20 dB, **c** 50 dB

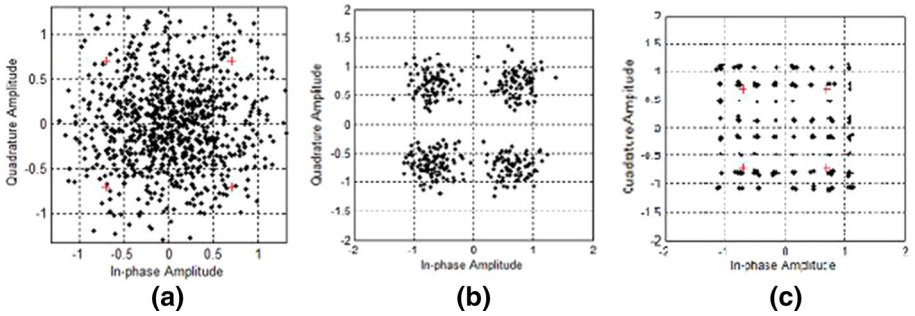

Fig. 11 CMA Equalizer output scatter plots (with STBC) over AWGN channel at different SNRs **a** 5 dB, **b** 20 dB, **c** 50 dB

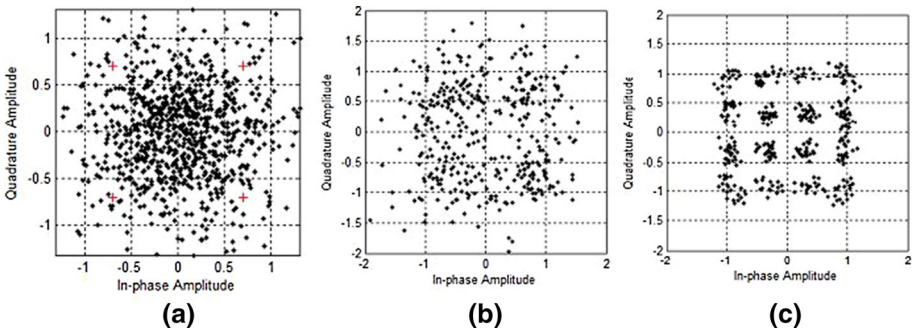

Fig. 12 CMA Equalizer output scatter plots (with STBC) over multi faded channel at different SNRs **a** 5 dB, **b** 20 dB, **c** 50 dB

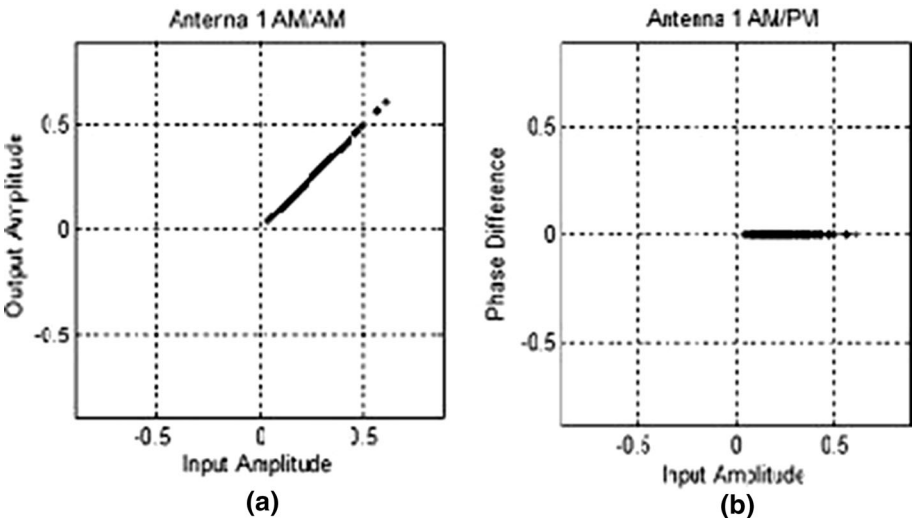

Fig. 13 An AM/AM and AM/PM plots at nonlinear output

7 Conclusion

In this paper, WiMAX physical layer is modeled with different channel equalizers and with STBC. Performance of physical layer is analyzed for both cases such as with STBC and without STBC. Scatter plots displayed the effect of each channel equalizer on WiMAX PHY. Results concluded the importance of channel equalizers for WiMAX PHY to achieve error free transmission. Results also concluded that blind equalizers performed well compared to decision feedback equalizers and linear equalizers.

References

1. Sampei, S. (1997). *Applications of digital wireless technologies to global wireless communications*. New York: Prentice Hall PTR.
2. Andrews, J. G., Ghosh, A., & Muhamed, R. (2007). *Fundamentals of WiMAX: Understanding broadband wireless networking*. New York: Pearson Education publications.
3. Dahlman, E., Parkvall, S., & Skold, J. (2013). *4G: LTE/LTE-advanced for mobile broadband*. London: Academic Press.
4. Zhu, H., & Wang, J. (2012). Chunk-based resource allocation in OFDMA systems :Part II: Joint chunk, power and bit allocation. *IEEE Transactions on Communications*, *60*(2), 499–509.
5. Poutanen, J., Salmi, J., Haneda, K., Kolmonen, V., & Vainikainen, P. (2011). Angular and shadowing characteristics of dense multipath components in indoor radio channels. *IEEE Transactions on Antennas and Propagation*, *59*(1), 245–253.
6. Huang, Y.-C., Tunali, N. E., & Narayanan, K. R. (2013). A compute-and-forward scheme for gaussian bi-directional relaying with inter-symbol interference. *IEEE Transactions on Communications*, *61*(3), 2704–2712.
7. Burse, K., Yadav, R. N., & Shrivastava, S. C. (2010). Channel equalization using neural networks: A review. *IEEE Transactions on Systems, Man, and Cybernetics, Part C: Applications and Reviews*, *40*(3), 352–357.
8. Merched, R. (2013). A unified approach to reduced-redundancy transceivers: Superfast linear and block-iterative generalized decision feedback equalizers. *IEEE Transactions on Signal Processing*, *61*(17), 4214–4229.
9. Gong, M., Chen, F., Yu, H., Lu, Z., & Hu, L. (2013). Normalized adaptive channel equalizer based on minimal symbol-error-rate. *IEEE Transactions on Communications*, *61*(4), 1374–1383.
10. Özen, A., Kaya, I., & Soysal, B. (2012). A supervised constant modulus algorithm for blind equalization. *Wireless Personal Communications*, *62*(1), 151–166.
11. Alamouti, S., & Tarokh, V. (2011). Transmitter diversity technique for wireless communications, Google Patents, US Patent 7,916,806, mar '29'.
12. Yang, D., Xu, C., Yang, L.-L., & Hanzo, L. (2011). Transmit-diversity-assisted space-shift keying for colocated and distributed/cooperative MIMO elements. *IEEE Transactions on Vehicular Technology*, *60*(6), 2864–2869.
13. Gulati, K., Evans, B. L., Andrews, J. G., & Tinsley, K. R. (2010). Statistics of co-channel interference in a field of poisson and poisson–poisson clustered interferers. *IEEE Transactions on Signal Processing*, *58*(12), 6207–6222.
14. Otaru, M. U., Zerguine, A., & Cheded, L. (2011). Channel equalization using simplified least mean-fourth algorithm. *Digital Signal Processing*, *21*(3), 447–465.
15. Leung, S.-H., & So, C. F. (2005). Gradient-based variable forgetting factor RLS algorithm in time-varying environments. *IEEE Transactions on Signal Processing*, *53*(8), 3141–3150.
16. Karimi-Ghartemani, M., & Iravani, M. R. (2002). A nonlinear adaptive filter for online signal analysis in power systems: Applications. *IEEE Transactions on Power Delivery*, *17*(2), 617–622.
17. Beres, E., & Adve, R. (2007). Blind channel estimation for orthogonal STBC in MISO systems. *IEEE Transactions on Vehicular Technology*, *56*(4), 2042–2050.
18. Chen, Z., et al. (2003). Performance of Alamouti scheme with transmit antenna selection. *IEEE Electronics Letters*, *39*(23), 1666–1668.
19. Zhang, Y., & Ge, S. S. (2005). Design and analysis of a general recurrent neural network model for time-varying matrix inversion. *IEEE Transactions on Neural Networks*, *16*(6), 1477–1490.

20. Yuan, J.-T., & Lin, T.-C. (2010). Equalization and carrier phase recovery of CMA and MMA in blind adaptive receivers. *IEEE Transactions on Signal Processing*, *55*(4), 3206–3217.
21. Khan, M. N., & Sabir G. (2008). The WiMAX 802.16 e physical layer model, IET international conference on wireless, mobile and multimedia networks.
22. Vaughan-Nichols, S. J. (2004). Achieving wireless broadband with WiMax. *Computer*, *37*(6), 10–13.

B. Siva Kumar Reddy received B.Tech (E.C.E) and M.Tech [VLSI Design (Very Large Scale Integrated circuits Design)] degrees from Jawaharlal Nehru Technological University, Hyderabad (JNTUH), India. Currently, he is working for doctorate in the field of wireless communications at National Institute of Technology, Warangal, India. He is an IEEE student member, ISTE (Indian Society for Technical Education) life time member and IDES (Institute of Doctors, Engineers and Scientists) member.

Dr. B. Lakshmi received B.Tech (E.C.E) from Nagarjuana university, M.Tech (EI) from NIT, Warangal, and Ph.D (VLSI Architectures) from I.I.T, Kharagpur, India. She is working as a faculty member in National Institute of Technology, Warangal since 1990. Her areas of interests are Digital System Design, Microprocessor Systems and VLSI Architectures. She is reviewer for Elsevier journals in VLSI area.